*Scientia Africana, Vol. 19 (No. 3), December, 2020. Pp 125-138* https://dx.doi.org/10.4314/sa.v19i3.9
*© Faculty of Science, University of Port Harcourt, Printed in Nigeria* *ISSN 1118 – 1931*

# SEISMIC-TO-WELL TIE OF A FIELD OF THE NIGERIAN DELTA

**[1]Inichinbia, S. and [2]Ahmed, A.L.**

[1]Department of Physics, University of Port Harcourt, Port Harcourt, Nigeria
[2]Department of Physics, Ahmadu Bello University, Zaria, Nigeria
Sonny.inichinbia@yahoo.com; sonny.inichinbia@uniport.edu.ng

*Received: 07-10-2020*
*Accepted: 16-10-2020*

## ABSTRACT

*This paper presents a rigorous but pragmatic and data driven approach to the science of making seismic-to-well ties. This pragmatic approach is consistent with the interpreter's desire to correlate geology to seismic information by the use of the convolution model, together with least squares matching techniques and statistical measures of fit and accuracy to match the seismic data to the well data. Three wells available on the field provided a chance to estimate the wavelet (both in terms of shape and timing) directly from the seismic and also to ascertain the level of confidence that should be placed in the wavelet. The reflections were interpreted clearly as hard sand at H1000 and soft sand at H4000. A synthetic seismogram was constructed and matched to a real seismic trace and features from the well are correlated to the seismic data. The prime concept in constructing the synthetic is the convolution model, which represents a seismic reflection signal as a sequence of interfering reflection pulses of different amplitudes and polarity but all of the same shape. This pulse shape is the seismic wavelet which is formally, the reflection waveform returned by an isolated reflector of unit strength at the target depth. The wavelets are near zero phase. The goal and the idea behind these seismic-to-well ties was to obtain information on the sediments, calibration of seismic processing parameters, correlation of formation tops and seismic reflectors, and the derivation of a wavelet for seismic inversion among others. Three seismic-to-well ties were done using three partial angle stacks and basically two formation tops were correlated.*

**Keywords:** seismic, well logs, tie, synthetics, angle stacks, correlation,

## INTRODUCTION

Seismic data are acquired in two-way-time, whereas well data are acquired in depth. The time-depth correlation is based on a table that ties seismic events in time with formation tops in depth. The table is presented as an interval velocity ($V_{int}$) profile derived from travel time differences between adjacent time-depth pairs $D_z$ and $D_t$:

$$V_{int} = D_z / D_t \quad (1)$$

Seismic-to-well ties are generally made with time-migrated data. Because as velocity tends to increase with depth, image points normally move up dip from the well. A data segment long enough to yield a bandwidth duration product of 25 or more (e.g. 0.5 s for 10 Hz - 80 Hz data) is needed to ensure a reliable seismic-to-well tie. A seismic-to-well tie compares seismic data around a well location with log data from the well. This requires at least a calibrated sonic log and calibrated density log for the generation of the synthetics. All other logs are optional and may not be used for the

generation of a composite borehole image along the well path. The location of the well is usually measured with great accuracy and serves as the basis for the well tie. The primary purpose of shooting a well is to obtain information which could be used in conjunction with seismic reflection data to determine depths, dips, and horizontal offsets of subsurface reflectors. In some cases, a time-depth relationship can be used directly. In seismic reflection, because reflecting boundaries are spaced much more finely in depth than the length of the reflected pulses, the degree of interference is generally severe and only the strongest reflectors or reflection complexes stand out in the reflection signal (White, 1997; White & Simm, 2003; Simm & White, 2002; Gratwick and Finn, 2005; Short & Stauble, 1967; Allouche *et al*., 2009; Inichinbia *et al*., 2014a).

**Location of the Study Area**

Figure 1 is the map of Niger Delta showing the study area. The field is located within licence oil mining lease OML 21 of the Greater Ughelli of the Niger Delta and is given a dummy name Amangi field. The Niger Delta lies between latitudes 4° N and 6° N and longitudes 3° E and 9° E.

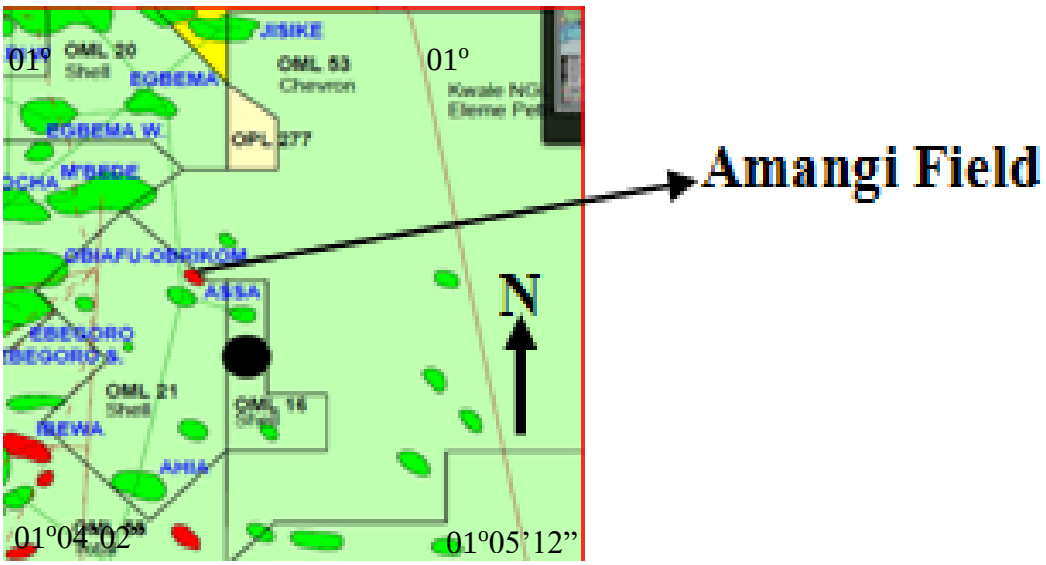


Figure 1. Map of Niger Delta showing the study area

## MATERIALS AND METHODS

Materials used in this work include, seismic data which is anisotropic 3D prestack depth migration data of four volumes (one full and three angle stacks- near, mid and far), log data from two wells with five logs each which include gamma ray, density, sonic, calliper and resistivity logs, and in addition well-1 has checkshot data. Checkshots are usually acquired in most exploration wells and are the basis of most well ties. Integrated sonic was for a more detailed velocity profile for the generation of the synthetics and time-depth relationship; sonic and density for generation of the synthetics, gamma ray and resistivity to highlight reservoir and pay, and calliper for borehole condition and quality control. Seismic and sonic velocities were calibrated against checkshots to obtain a proper merge. However, a series of simple log

*Scientia Africana, Vol. 19 (No. 3), December, 2020. Pp 125-138* https://dx.doi.org/10.4314/sa.v19i3.9
*© Faculty of Science, University of Port Harcourt, Printed in Nigeria* *ISSN 1118 – 1931*

transformations can normalize several logs to a common shale response, enabling coherent display of multiple logs in a single image and best results are obtained when coherent logs are adjacent. In the well log editor panel, a default order of Gamma ray, Density, Neutron, Shear, and Sonic is preferred. Some softwares used include Jason Geoscience workbench, Petrel 2.0, Techlog, and Savior.

## RESULTS AND INTERPRETATION

A detailed but concise description of the results and their interpretations is given as follows:

### Well Log Editing

Figure 2 is the well editor panel displaying some log curves obtained from well-1. From left to right, the first panel is the measured depth in feet, the second panel displays the reservoirs (horizons), the third panel contains both the gamma ray (API unit) and calliper curves, the fourth panel is the resistivity curve, the fifth panel displays two density curves- the log curve of the measured density (blue) overlain by edited density curve (purple) by the quantitative interpretation (QI) unit of the Shell Petroleum Development Company (SPDC) of Nigeria Limited. The sixth and last panel displays measured sonic log (blue) and the QI edited sonic. Quality Control (QC) checks were done on the well logs for problems especially with washout and invasion, which could result in poor sonic and density logs. Also, QC check was done on the calliper log in relation to areas where there is a poor tie. These problems could actually cause issues when modeling shear velocity ($V_s$) from sonic velocity ($V_p$) if there is a problem with the $V_p$.

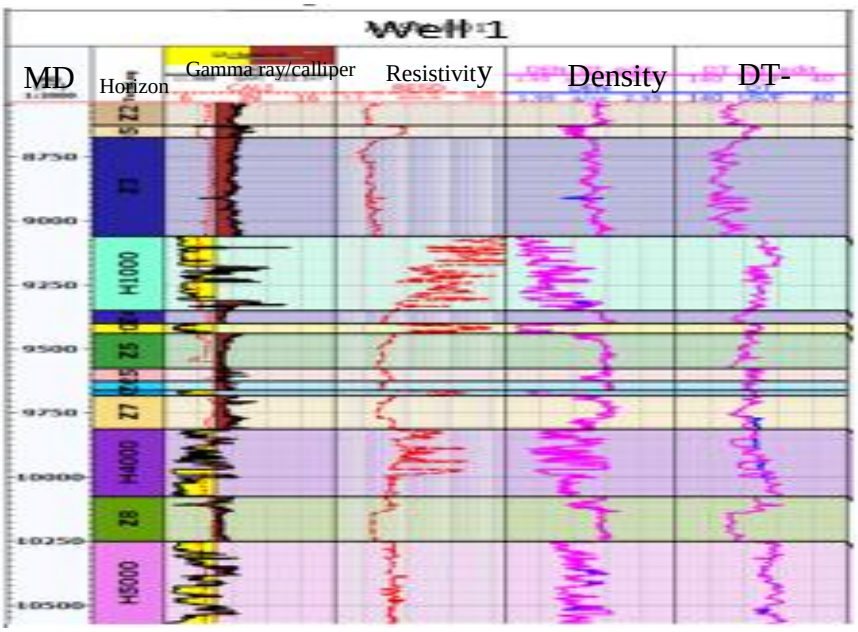


Figure 2. Well Log Editing

### Log Display

A seismic-to-well tie usually requires many logs. For example, integrated sonic log for the time-depth conversion, sonic and density logs for generation of the synthetic, gamma ray and resistivity logs to highlight

reservoir and pay, and calliper log for borehole condition and quality control. In general, too much information is required for a comprehensive display on top of the seismic and the synthetic.

Figure 3 is the well panel displaying the QI edited logs of Well-1. From left to right of the panel are measured depth TVDSS (ft), reservoirs (H1000, H4000) of interest in this work, gamma ray and calliper curves, water saturation (v/v), density (g/cm$^3$), sonic (µs/ft) and acoustic impedance (AI). The AI of each layer is derived from the density and sonic log. Understanding acoustic log response is very important in interpreting rock properties. H1000 and H4000 are prominent anomalies on all the logs.

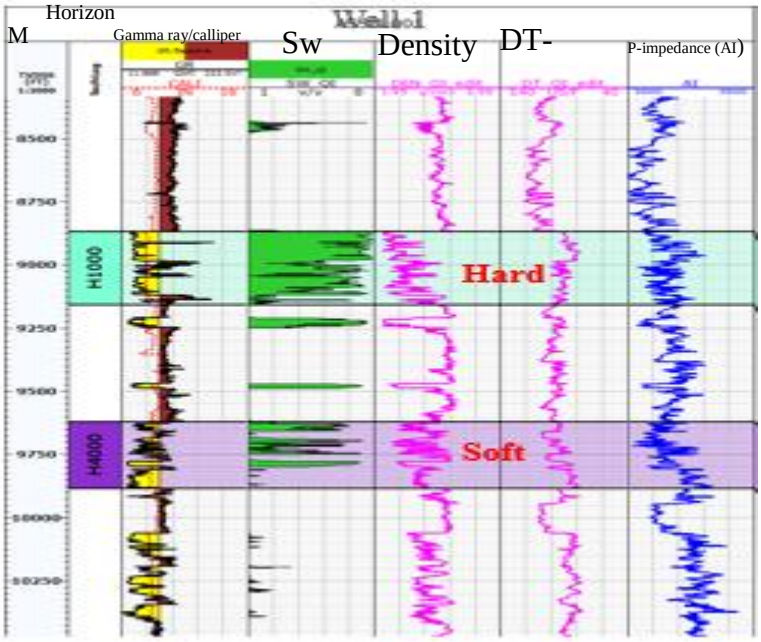


Figure 3. Log Signatures of Well-1

It is noteworthy that from the perspective of analysing the seismic response of a reservoir, log editing and conditioning is of paramount importance.

**Modelling of Shear wave**

Generally, the sonic logs are modelled with expected changes and the resulting synthetic traces are examined to determine the characteristics of the sands' porosity (or any other feature) to be identified on the stacked traces. The synthetic shear sonic was modelled from an in-house package in savior called AVOModel since we do not have a true shear log ($V_s$) and was imported into Jason as S-velocity (µs/ft). In Figure 4, the modelled logs are displayed as red curves ($V_s$, $V_{sh}$, and $V_p/V_s$), whereas the measured logs are displayed as purlple curves (density, $V_p$). Water saturation, porosity, and volume of shale logs are also displayed in the panel. Figure 5 is the workflow for the synthesis of the sonic responses.

*Scientia Africana, Vol. 19 (No. 3), December, 2020. Pp 125-138* https://dx.doi.org/10.4314/sa.v19i3.9
*© Faculty of Science, University of Port Harcourt, Printed in Nigeria* *ISSN 1118 – 1931*

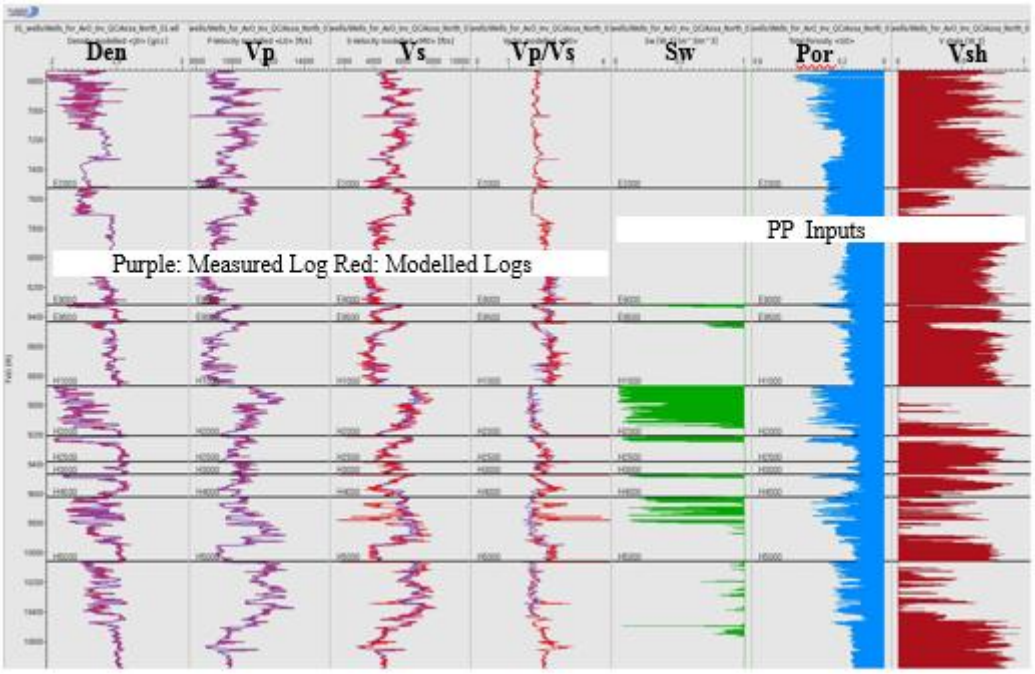


Figure 4. Petrophysical modelling of shear velocity

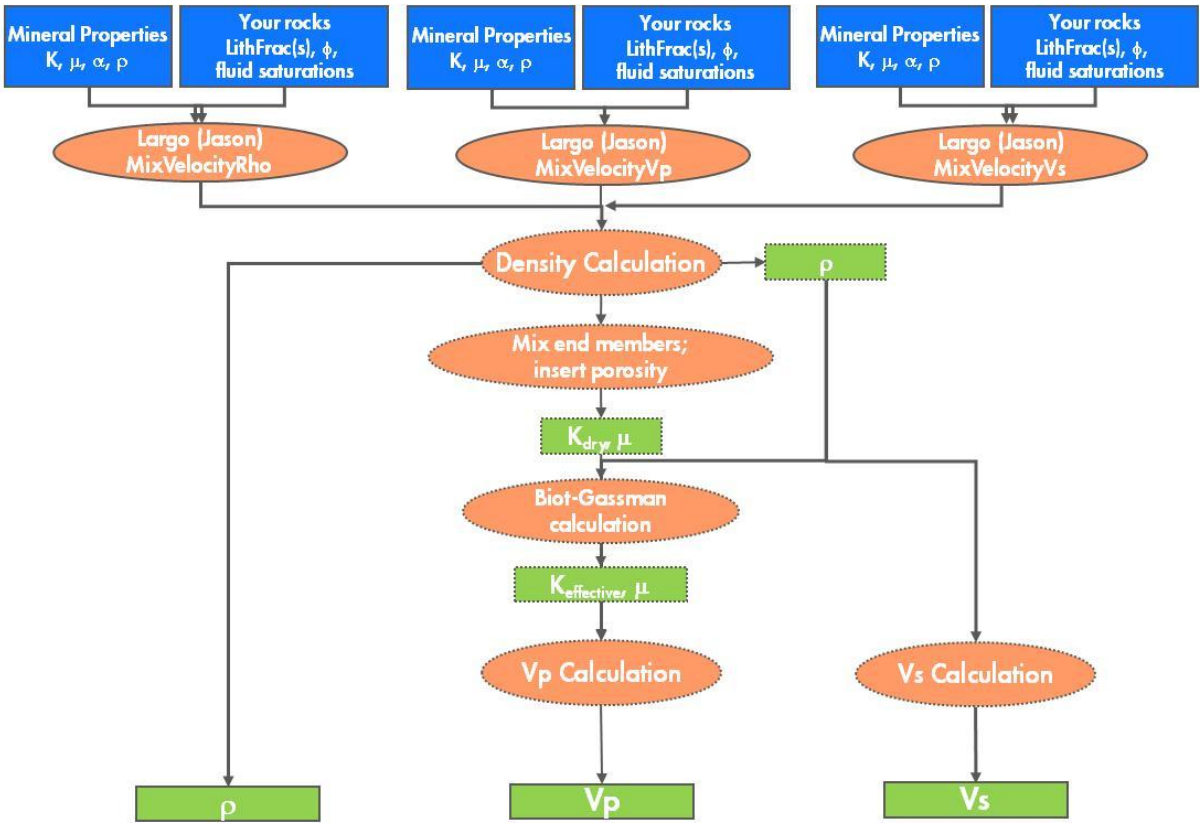


Figure 5. Workflow for modelling the synthesis of sonic responses by rock physics

**Seismic data analysis**

The seismic survey covers an area of 20 x 17.5 $km^2$ with inline spacing 25 m and crossline spacing 25 m (see Figure 5). Note that a seismic survey records acoustic wave fronts reflected in the subsurface. Actually, seismic waves are reflected at acoustic impedance boundaries. The reflection strength depends on the relative magnitude of the impedance contrast between two layers:

$$R = (AI_2 - AI_1) / (AI_2 + AI_1) \quad (2)$$

where, R = reflection coefficient

$AI_1$ = bulk $density_1$ * compressional $velocity_1$

$AI_2$ = bulk $density_2$ * compressional $velocity_2$

Reflection coefficients at the interfaces are resampled from reflection depth to reflection time. The recorded data were sorted on common-mid-point (CMP), and the travel time differences along different ray paths are converted into stacking velocities for signal processing. The seismic data were processed into an anisotropic 3D prestack depth migrated volume, consisting of a full volume or full stack and three (near, mid, and far) angle stacks, sampling interval was 4 ms.

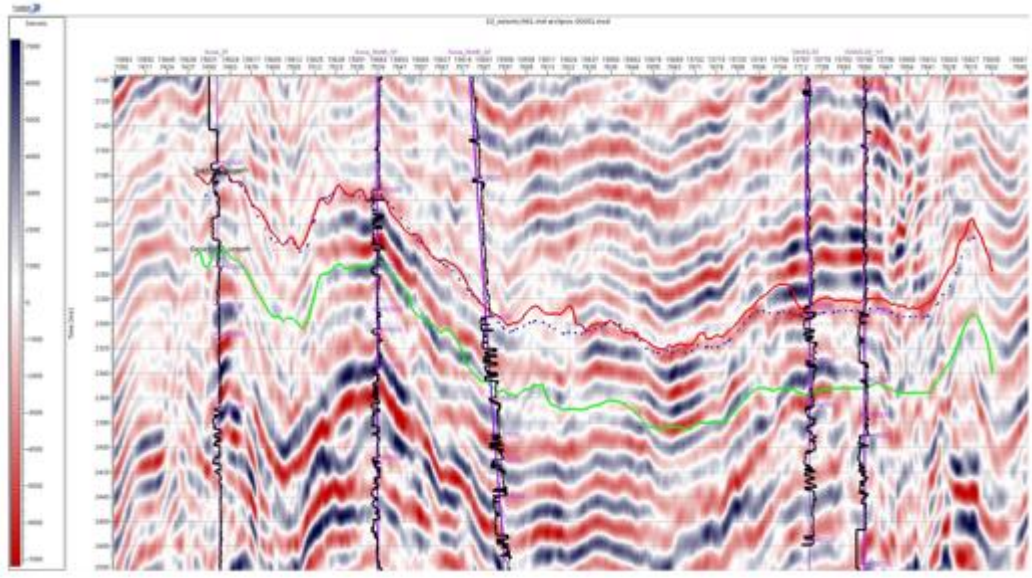

Figure 5. Processed seismic full volume overlain with logs from the five wells in the field. The section shows the horizon H1000 captured top (red) and base (green).

Since, stacking velocities are unsuitable for time-depth conversion they were converted to interval velocities, using the Dix formula:

$$Vint_n = sqrt( (Vstk_n^2 t_n - Vstk_{n-1}^2 t_{n-1}) / (t_n - t_{n-1}) ) \quad (3)$$

where $Vstk_{n-1}$ and $Vstk_n$ are the stacking velocities from the reflectors above and below the $n_{th}$ interval, with arrival times $t_{n-1}$ and $t_n$. With properly handled static and dynamic corrections and deconvolution (see Figure 6), the stacking process improved the signal-to-noise ratio of recorded data (see Figure 7) to such an extent that it became realistic to analyze amplitude (see Figure 8) and frequency characteristics (see Figre 9) of particular reflections. The signal processing was

*Scientia Africana, Vol. 19 (No. 3), December, 2020. Pp 125-138* https://dx.doi.org/10.4314/sa.v19i3.9
*© Faculty of Science, University of Port Harcourt, Printed in Nigeria* *ISSN 1118 – 1931*

followed by velocity analysis for prestack depth migration (PreSDM). This was informed by the reason that seismic data may be distorted by a complex overburden so, it was migrated into an accurate image at the correct location.

Figure 7 is the panel displaying the angular subdivisions (near, mid and far angle stacks) of the full anisotropic 3D prestack depth migrated seismic volume with the wells on the field inserted.

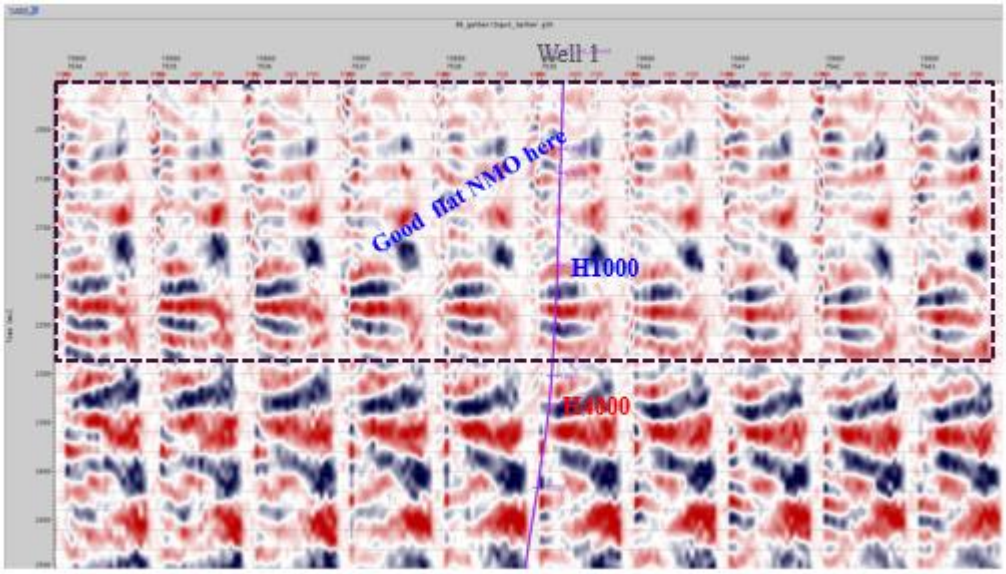


Figure 6. Normal moveout (NMO) corrected and flattened Gathers around Well-1 location, the seismic is overlain with Well-1 (from Inichinbia *et al.*, 2014b)

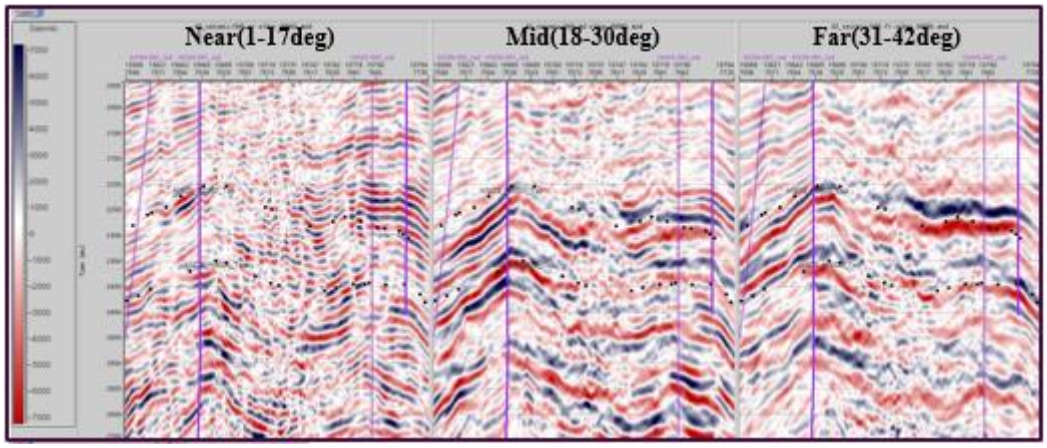


Figure 7. Quality control checks of the three angle stacks.

Figure 8 shows how the three angle stacks are aligned in time. The amplitudes of the mid stack seemed clipped and they appear too bright compared to near angle stack and the far angle stack. On the right end of the panel, the red curve is a gamma ray log while the blue curve is acoustic impedance log derived from convolution of density log with the sonic log. The amplitude scaling is derived in a gate of one second across the entire panel and the gate is centered on the sonic and density logs to allow compatible scaling of the synthetics. The gate is also used to derive the amplitude spectrum and

dominant frequency of the seismic. The spectrum is derived from autocorrelation of seismic traces and will be used to generate synthetics that match the seismic signature.

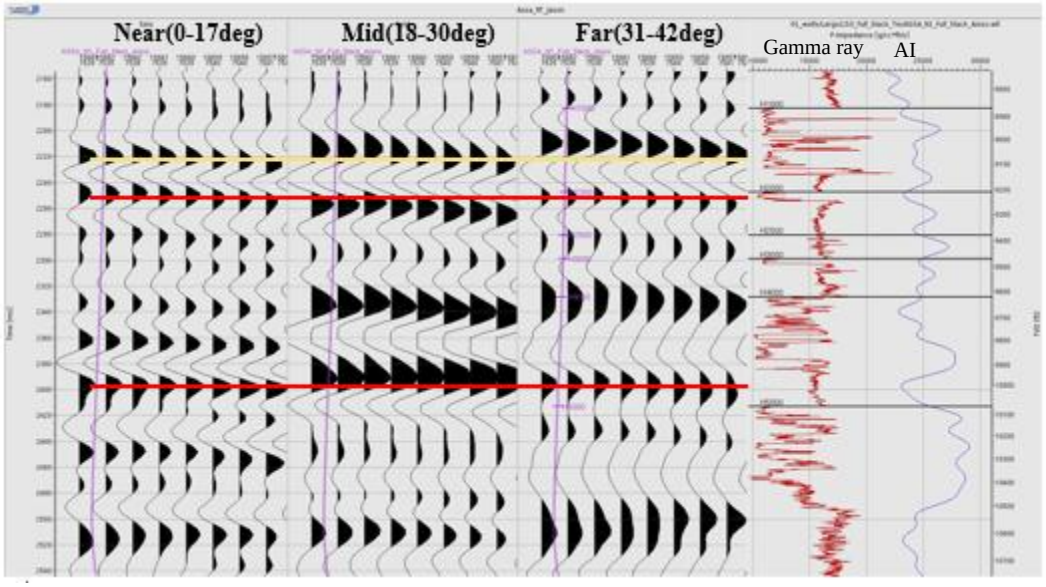


Figure 8. Quality control checks of the three angle stacks (0 - 42 degrees reflection, from Inichinbia *et al*., 2014b)

Figure 9 is the panel displaying the amplitude and frequency distribution of the three angle stacks colour coded to amplitude spectrum. Here, the near angle stack ranges from 1.0$^{o}$ to 17$^{o}$. Frequencies go down from near to mid to far as expected and the low frequency signals are missing in the near angle stack.

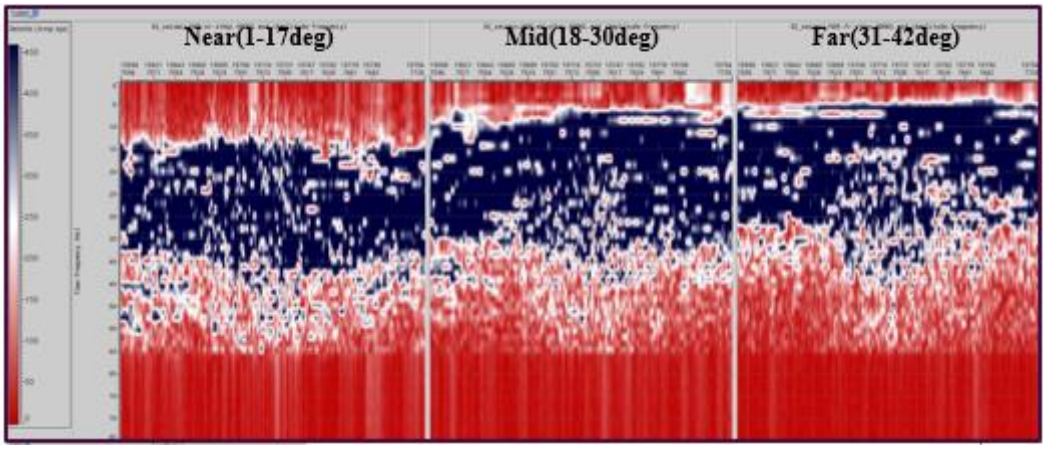


Figure 9. Amplitude and frequency distribution of the angle stacks at 2000 ms - 2700 ms window colour coded with the amplitude spectrum.

The amplitude spectrum of the seismic was derived from autocorrelations in an area around the borehole. The spectrum was derived in a time gate of one second (centered on the synthetic) across all the traces in the selected traverse. The dominant frequency is derived from the number of zero crossings per second and is used to auto size some other parameters. For example, wavelet lengths and correlation lags are

*Scientia Africana, Vol. 19 (No. 3), December, 2020. Pp 125-138* https://dx.doi.org/10.4314/sa.v19i3.9
*© Faculty of Science, University of Port Harcourt, Printed in Nigeria* *ISSN 1118 – 1931*

defined in multiples of the dominant cycle time (or number of cycles).

From the available evidence (see Figure 10) got from the logs of Well-1, the reflection signals are reliable up to 42 degrees in the H1000 and 52 degrees in the H4000 reservoirs respectively. This informed the subdivision of the full seismic volume into angle stacks such as the near angle stack ($0^o$ – $17^o$), mid angle stack ($18^o$ – $30^o$) and far angle stack ($31^o$ – $42^o$).

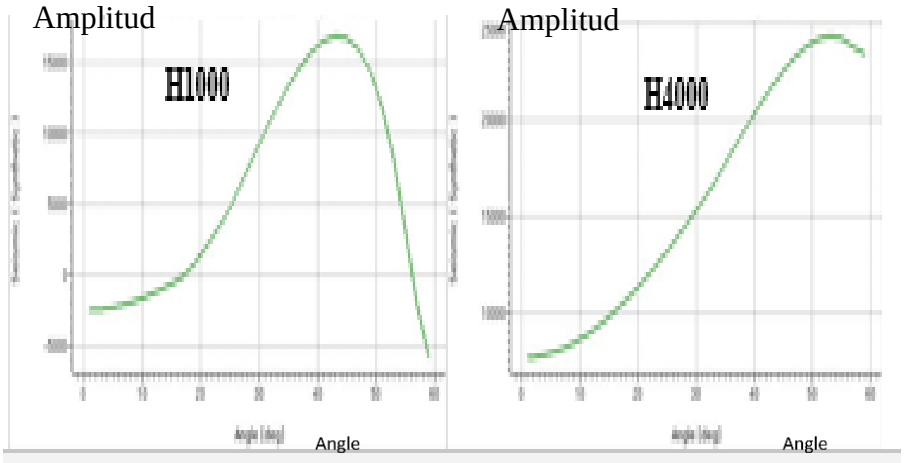


Figure 10. Amplitude variation with angle (AVA) synthesis of Well-1.

**Wavelet Generation**

An initial (Ricker) wavelet was derived from the seismic estimate wavelet amplitude and phase spectra. The wavelet was scaled to get polarity from distinct event. Also, the wavelet was tapered at three times the dominant cycle time, and a low cut was applied to eliminate any direct current (DC) bias. The purpose of the taper was to suppress the non relevant side lobes of the wavelet. Convolution of the wavelet with the impedance contrasts from the well yielded an initial synthetic, and the dominant frequency of the synthetic was compared with the dominant frequency of the seismic irrespective of the phase, polarity, and time shifts. The initial synthetic presumed a flat earth spectrum and was too high of a frequency. The wavelet was tapered and coloured with an exponential earth spectrum until the signature of the synthetic matched the seismic. The wavelet taper effectively smoothens the spectrum, whereas the earth color effectively tilts the spectrum. The shape of the spectrum remains very similar and the match between synthetic and seismic was judged from the dominant frequencies. The wavelet spectrum is not exactly the same as seismic spectrum, but it is approximately over the same range as seismic spectrum. The wavelets are good and consistent. The estimated wavelet is displayed in Figure 11.

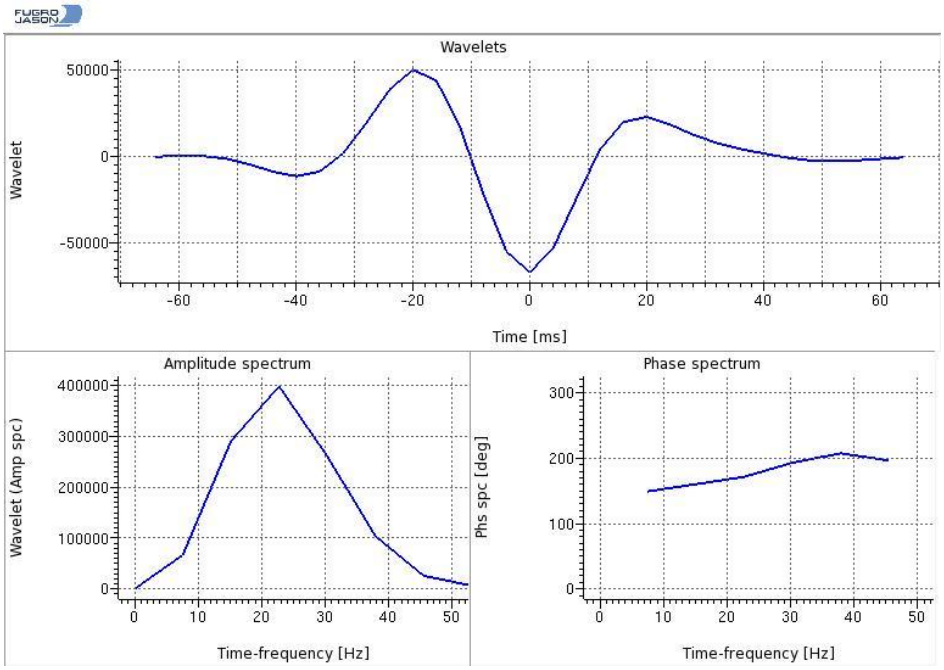


Figure 11. Wavelet amplitude phase spectrum

**Synthetics generation**

The reflection time series is convolved with a wavelet to generate the synthetic seismogram that is compared with the actual seismic. Acoustic impedance contrasts are stationary in depth, and hence, synthetic wiggles are stationary in depth and not in time. The initial synthetic was zero phase, but the polarity and phase was flipped to match local polarity conventions. The synthetic is displayed in depth as wiggle traces along the borehole. Errors in timing of the well-log synthetic seismogram are more damaging than errors in amplitude, particularly at higher frequencies. Log calibration using times from a checkshot optimises the timing of seismic and well log ties. Some editing and conditioning of the logs was performed before constructing the synthetic seismogram from them.

**Seismic and Synthetics correlation**

Now we need to do our seismic-to-well tie after we have made an initial Earth model and created our impedance log data which is very important. Seismic-to-well tie was done in Jason Geoscience Workbench to tie and create a wavelet. The quality of a seismic-to-well tie was judged from the correlation between the synthetic and the seismic. The correlation was repeated for a series of time shifts to investigate time and phase errors. The maximum correlation lag was restricted to 2.5 "cycle skips" up or down. However, for a perfect well tie, the correlation peaks were centered about zero time lag. The correlations are skewed towards negative values. Correlation skewness is associated with phase differences between the seismic and the synthetic. Thus, in mathematical terms:

Skewness (Xcorrelation) = cosine (Phase Difference) . . (4)

Thus, the correlation panel is predominantly negative. That is, the correlations are skewed towards negative values. Both the seismic and the synthetic have the same

*Scientia Africana, Vol. 19 (No. 3), December, 2020. Pp 125-138* https://dx.doi.org/10.4314/sa.v19i3.9
*© Faculty of Science, University of Port Harcourt, Printed in Nigeria* *ISSN 1118 – 1931*

polarity, and the phase difference is minimal.

Figures 12, 13 and 14 display the seismic-to-well tie panels for the near, mid and far angle stacks of Well-1 respectively. From left to right of each panel is the cross correlation, wavelet for each angle volume, seismic, synthetic, correlation, drift, and gamma ray log (red), calibrated acoustic impedance log (blue) and calibrated sonic log (purple) respectively. Well-1 (purple) is also inserted in the panel. Figure 12 shows a gas sand with nonzero phase synthetic on top of the seismic. The top of the sand H1000 (red horizon) is a hard reflector while the top of the sand H4000 (green horizon) is a soft reflector and the well tie appears simple. The hard reflections are caused by increases in acoustic impedance downwards across a boundary. The seismic image is slightly shallower than the synthetic; a minor time-depth issue that can be resolved with a static shift. The correlation panel contains important diagnostics to resolve time-depth and phase issues. The synthetic-seismic correlation of a proper seismic-to-well tie peaks at lag time zero and has balanced side lobes. This is clearly not the case in this panel. In fact, the correlations are predominantly positive, suggesting same polarity between the seismic and the synthetic.

In the Nigerian Delta, sometimes phase differences between the synthetic and seismic are easily confused with time shifts and are difficult to resolve, because of repetitive geology and monochromatic seismic, loop skips, polarity reversals and cross correlations cluttered with side lobes. Phase differences were minimized when correlation peaks coincides with peaks on the correlation envelope, that is to say when the product of x***correlation*envelop*** reaches its peak.

where xcorrelation = shifted cross correlation between the seismic and the synthetic.

envelop = envelope of the shifted cross correlation = square root ($xcor^2 + ycor^2$)

ycorrelation = imaginary correlation between -90º Phase shift (seismic) and synthetic

This product enhances coincident peaks and suppresses side lobes, as can be seen on the panel. The impact is quite dramatic. The clutter on the correlation panel is virtually gone after enhancement with the correlation envelope. The enhanced correlation also provided a basis for estimation of the phase differences between the seismic and the synthetic that is impartial to time-depth errors, as long as the errors are within a reasonable range, (for instance, one cycle skip up or down) between seismic and synthetic. In general, there is too much information for a comprehensive display on top of the seismic and the synthetic.

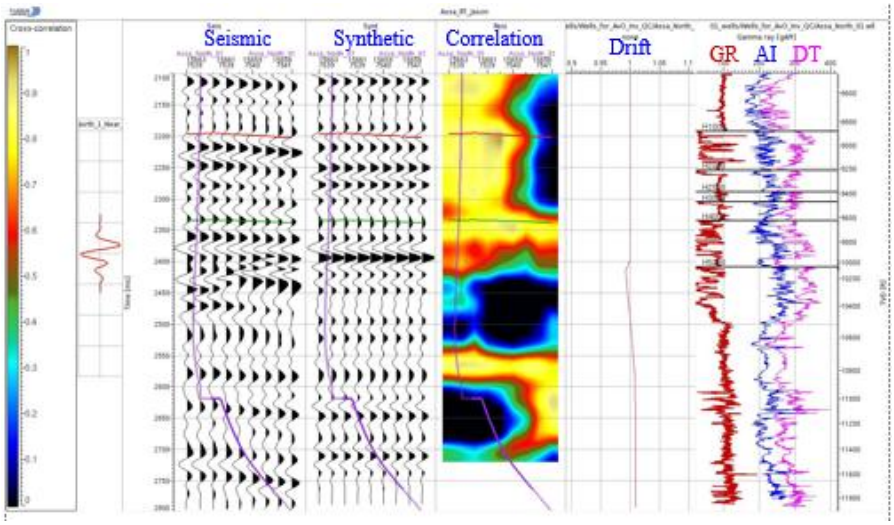


Figure 12. Seismic-to-well tie of the near stack for Well-1

Figure 13 is the seismic-to-well tie of the mid angle stack of Well-1. The panel shows a gas sand with zero phase synthetic on top of the seismic. The top of the sand H1000 (red) is a hard reflector while the top of the sand H4000 (green) is a soft reflector and the seismic-to-well tie equally appears simple. The seismic image is slightly shallower than the synthetic; a minor time-depth issue that can be resolved with a static shift. The correlation is positive suggesting same polarity between the seismic and the synthetic.

Figure 14 is the panel of the well-to-seismic tie of the far angle stack of Well-1. The top of the sand H1000 (red) is a hard reflector while the top of the sand H4000 (green) is a soft reflector and the seismic-to-well tie equally appears simple. The seismic image is slightly shallower than the synthetic; a minor time-depth issue that can be resolved with a static shift. There is no balanced side lobes, thus, suggesting opposite polarity between seismic and the synthetic at the H1000, but exhibits same polarity between the seismic and the synthetic at the H4000.

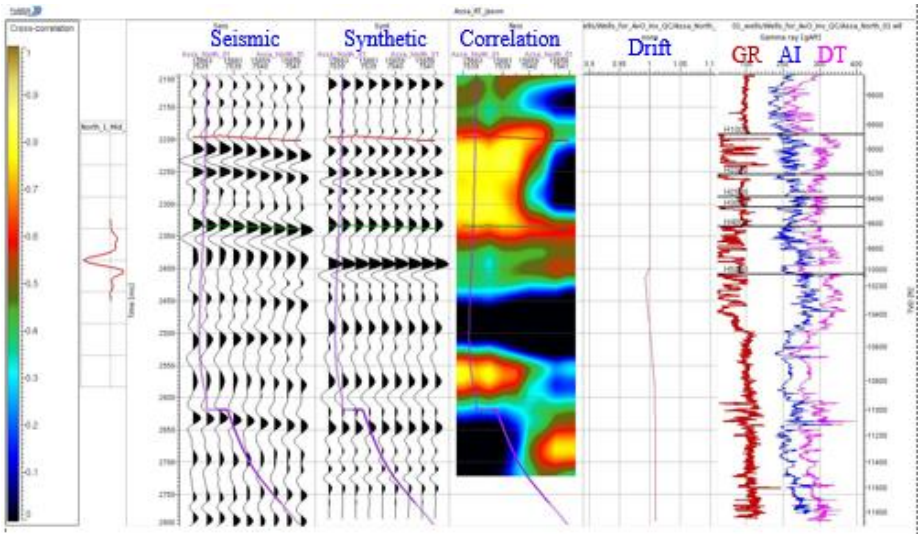


Figure 13. Seismic-to-well tie of the mid stack of Well-1

*Scientia Africana, Vol. 19 (No. 3), December, 2020. Pp 125-138* https://dx.doi.org/10.4314/sa.v19i3.9
*© Faculty of Science, University of Port Harcourt, Printed in Nigeria* *ISSN 1118 – 1931*

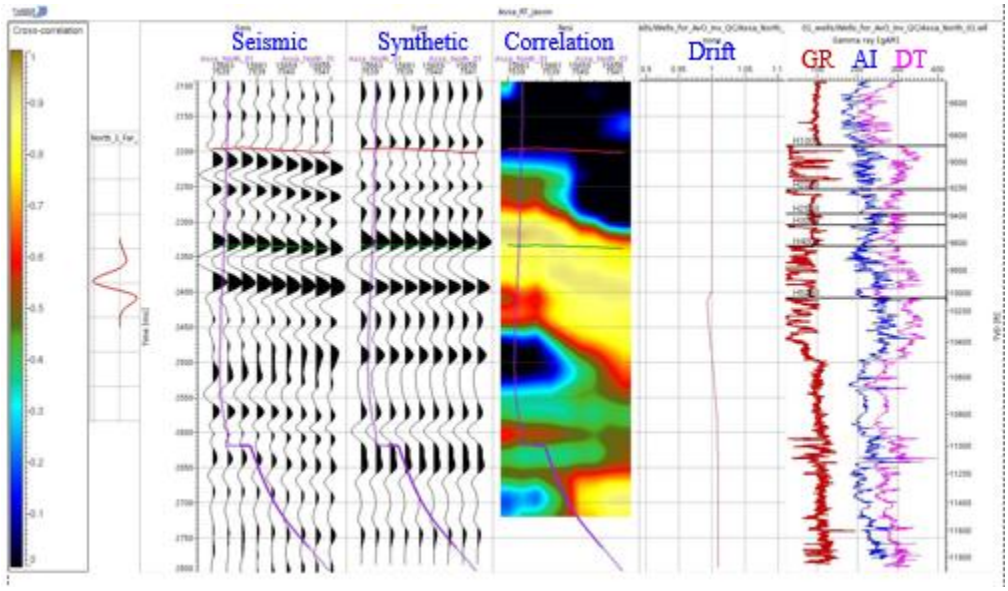


Figure 14. Seismic-to-well tie of the far angle stack of Well-1

Quality Control (QC) checks were performed on the seismic-to-well tie panel to measure how much change has been applied to the time-depth relationship. For instance, the slowness drift (relative) shows the percentage of velocity change as a result of stretching and squeezing. Time drift (absolute) shows the change in time-depth relationship in milliseconds. Maximum drift from the original time-depth profile was set at default of 1.0 ms while maximum change between adjacent time-depth pairs was set at default of 5.0 %. The outcome of stretch and squeeze is that the synthetic is modified based on the new time-depth relationship and the slowness curve is recalculated to show the changes. Thus, immediate modification of the slowness curve is a QC feature as it allows us to determine if the applied stretch and/or squeezing results in geologically reasonable sonic value. Correction of the synthetic phase may not yield an optimal well tie. Residual phase differences may impair the skewness of the cross correlation, which can be resolved by adjusting the phase of the seismic.

## DISCUSSION

Seismic-to-well tie is a very important part of the seismic interpreter's business as it provides him/her a means to correctly identify horizons to pick, and estimate the wavelet for inverting seismic data to acoustic impedance among others. It is not possible without performing a quantitative seismic-to-well tie to confidently assume that knowing the polarity convention necessarily implies that the shape of the wavelet is also known, and accurate timing in particular can be found only from seismic-to-well ties.

The prerequisites for a close tie between the well log synthetic seismogram and the seismic data volume are accurate sonic and density logs and good quality seismic data. QC of the well log and seismic data, timing and log calibration, seismic-to-well tie location, seismic bandwidth and signal-to-noise ratio, and the use of seismic-to-well tie diagnostics all play an important part in making close seismic-to-well ties. Seismic-to-well ties have become fundamental to the interpretation of modern seismic data.

Finally, through this rigorous but pragmatic and data driven approach to seismic-to-well ties, horizons picked have been related directly to a well log and they have provide a means of estimating the wavelet needed to invert seismic data to impedance and to rock property indicators.

**Acknowledgements**

The authors are grateful to Prahlad Basak, Francesca I. Osanyande, Dike Robinson and Temitope Jegede for their invaluable contributions to the success of this work. We also appreciate the assistance of colleagues of the department of Physics. We are also grateful to the members of staff of the Geosolutions section and Shell Petroleum Development Company (SPDC) of Nigeria Limited for providing the data.

**REFERENCES**

Allouche, P., Thore, P. and Monnerie, T. (2009) *Towards a better seismic to well tie in complex media. International Exposition and Annual Meeting, Houston, Society of Exploration Geophysicists, 1870 – 1874.*

Gratwick, D. and Finn, C. (2005) *What's important in making far stack well-to-seismic ties in West Africa? The Leading Edge, **24**(7), 739 – 745.*

Inichinbia, S., Sule, P.O., Ahmed, A.L. and Hamza, H. (2014a) *Well-to-seismic tie of Amangihydrocarbon field of the Niger Delta of Nigeria. IOSR Journal of Applied Geology and Geophysics, **2**(2), Ver. I., 97 - 105.*

Inichinbia, S., Sule, P.O., Ahmed, A.L. and Hamza, H. (2014b) *AVO inversion and Lateral prediction of reservoir properties of Amangi hydrocarbon field of the Niger Delta area of Nigeria. IOSR Journal of Applied Geology and Geophysics 2(2), Ver. II., 08 – 17.*

Short, K.C. and Stauble, A.J. (1967) *Outline of geology of Niger Delta. The American Association of Petroleum Geologists Bulletin, **51**(5), 761 – 799.*

Simm, R. and White, R. (2002) *Phase, polarity and the interpreter's wavelet first break volume **20**(5), 277 – 281.*

White, R. and Simm, R. (2003) *Tutorial: Good practice in well ties. First Break, **21**(5), 75 – 83.*

White, R.E. (1997) *The accuracy of well ties: practical procedures and examples, Expanded Abstract RC1.5, 67th SEG Meeting, Dallas.*